Role of the Ω-Loop in the Activity, Substrate Specificity, and Structure of Class A β-Lactamase[†,‡]

Soojay Banerjee,[§] Ursula Pieper,[§] Geeta Kapadia,[§] Lewis K. Pannell,[||] and Osnat Herzberg*[,§]

Center for Advanced Research in Biotechnology, University of Maryland Biotechnology Institute, 9600 Gudelsky Drive, Rockville, Maryland 20850, and Laboratory of Bioorganic Chemistry, National Institute of Diabetes and Digestive and Kidney Diseases, National Institutes of Health, Bethesda, Maryland 20892

Received August 26, 1997; Revised Manuscript Received November 13, 1997

ABSTRACT: The structure of class A β-lactamases contains an Ω-loop associated with the active site, which carries a key catalytic residue, Glu166. A 16-residue Ω-loop deletion mutant of β-lactamase from *Staphylococcus aureus* PC1, encompassing residues 163−178, was produced in order to examine the functional and structural role of the loop. The crystal structure was determined and refined at 2.3 Å, and the kinetics of the mutant enzyme was characterized with a variety of β-lactam antibiotics. In general, the wild-type β-lactamase hydrolyzes penicillin compounds better than cephalosporins. In contrast, the deletion of the Ω-loop led to a variant enzyme that acts only on cephalosporins, including third generation compounds. Kinetic measurements and electrospray mass spectrometry revealed that the first and third generation cephalosporins form stable acyl-enzyme complexes, except for the chromogenic cephalosporin, nitrocefin, which after acylating the enzyme undergoes hydrolysis at a 1000-fold slower rate than that with wild-type β-lactamase. Hydrolysis of the acyl-enzyme adducts is prevented because the deletion of the Ω-loop eliminates the deacylation apparatus comprising Glu166 and its associated nucleophilic water site. The crystal structure reveals that while the overall fold of the mutant enzyme is similar to that of the native β-lactamase, local adjustments in the vicinity of the missing loop occurred. The altered β-lactam specificity is attributed to these structural changes. In the native structure, the Ω-loop restricts the conformation of a β-strand at the edge of the active site depression. Removal of the loop provides the β-strand with a new degree of conformational flexibility, such that it is displaced inward toward the active site space. Modeled Michaelis complexes with benzylpenicillin and cephaloridine show that the perturbed conformation of the β-strand is inconsistent with penicillin binding because of steric clashes between the β-lactam side chain substituent and the β-strand. In contrast, no clashes occur upon cephalosporin binding. Recognition of third generation cephalosporins is possible because the bulky side chain substituents of the β-lactam ring typical of these compounds can be accommodated in the space freed by the deletion of the Ω-loop.

The serine β-lactamases utilize an active site serine residue to hydrolyze the β-lactam amide bond typical of β-lactam antibiotics. There are three sequence-based classes of serine β-lactamases, of which the class A enzymes are plasmid-encoded monomeric molecules of approximately 250 amino acid residues in length (*1*). The hydrolysis of the β-lactam amide bond proceeds via a mechanism that involves an acyl-enzyme intermediate at the O^{γ} atom of an invariant serine residue that acts as the nucleophile (*2*−*5*). Following the consensus numbering scheme of Ambler et al. (*6*), this serine is located at position 70.

In addition to Ser70, other key active site residues revealed by a number of high-resolution crystal structures of the enzyme from various organisms include Lys73, Glu166, Lys234, and Ser130 (*7*−*13*). The role of these residues and the mechanistic similarity to the class C serine β-lactamases have been the subject of much discussion (*7*, *13*−*20*). An analogy to the mechanism of the serine proteases can be drawn because of the involvement of the active site serine and the possible role of an oxyanion hole in catalysis (*7*). In contrast to serine proteases, it is now generally accepted that the acylation and deacylation machineries differ, with Glu166 playing a major role only during deacylation (*7*, *13*, *19*, *21*−*25*).

Glu166 is located on an Ω-loop (Figure 1) comprising residues 163−178 (*7*, *8*). Two structural features present in the *Staphylococcus aureus* PC1 β-lactamase led to the proposal that the loop may be marginally stable even though it is well ordered in the crystal structure (*21*, *25*). First, the loop is not well packed against the rest of the molecule, with several internal water molecules separating it from the core. Second, the peptide bond between the catalytic residue Glu166 and the following Ile167 is a *cis* bond. Non-proline *cis* peptides are energetically unfavorable and are rare in proteins (*26*). The high-resolution crystal structures of class A β-lactamases from other organisms contain a proline *cis*

[†] Supported by NIH Grant RO1-AI27175.

[‡] The crystal structure coordinates have been deposited in the Brookhaven Protein Data Bank (entry code 1OME).

* To whom correspondence should be addressed (telephone, 301-738-6245; fax, 301-738-6255; e-mail, osnat@carb.nist.gov).

[§] University of Maryland Biotechnology Institute.

[||] NIDDKD, National Institutes of Health.

S0006-2960(97)02127-2 CCC: $15.00
Published on Web 02/20/1998

FIGURE 1: Overall fold of β-lactamase, highlighting the Ω-loop (gold) and three catalytic residues, Ser70, Lys73, and Glu166 (red).

peptide, and no internal water molecules are present between the Ω-loop and the remaining structure (*9*−*13*).

Three invariant electrostatic interactions help maintain the structural integrity of the Ω-loop and therefore enzyme activity. These are (a) the interaction between the side chains of the catalytic Lys73 and Glu166, (b) the interaction between Arg164 and Asp179, and (c) the interaction of the CO and NH_2 groups of the Asn136 side chain with the main chain NH and CO groups of Glu166, respectively. For the *S. aureus* enzyme, it was shown that removing one of these interactions at a time impaired enzyme activity and stability. In the P54 mutant β-lactamase, Asp179 is replaced by Asn, eliminating the possibility of forming a salt bridge with Arg164. Stopped-flow kinetic measurements showed that the mutant enzyme is deacylation defective, and the crystal structure revealed that part of the Ω-loop including Glu166 is disordered (*21*). Urea gradient polyacrylamide gel electrophoresis, together with circular dichroism and sedimentation velocity experiments, indicated that the folding of the P54 mutant enzyme is incomplete also in solution (*27*). The mutation N136A removes the interaction that helps stabilize the non-proline *cis* peptide bond. The mutant enzyme is deacylation impaired and forms stable acyl-enzyme adducts with cephalosporins but not with penicillins (*25*). The stability of the N136A β-lactamase is reduced by 2 kcal/mol compared with the wild-type enzyme.

The current study examines the impact of the deletion of the Ω-loop on the activity and structure of the enzyme. The results support the proposed role for the Ω-loop in enzyme structure and function and reveal that, in addition, the β-lactam recognition profile typical of the class A β-lactamases has been altered such that the mutant enzyme forms acyl-enzyme complexes with cephalosporins, including third generation cephalosporins, but not with penicillins. For brevity, the Ω-loop deletion β-lactamase is referred to as the Ω-deletion enzyme.

MATERIALS AND METHODS

Mutagenesis, Expression, and Protein Purification. The Ω-deletion β-lactamase from *S. aureus* PC1 was cloned, expressed in *Escherichia coli* TG1, and purified following a protocol similar to that in Zawadzke et al. (*28*), with modifications described in Zawadzke et al., (*19*). The four-primer overlap−extension method (*29*) was used to produce the mutant protein from the β-lactamase gene on pTS32 (*bla*Z). The two external primers were oligonucleotides LZBAMHI (5′-GTCCGGCGTAGAGGATCCGGAATTCT-CATG-3′) and TSHIND3 (5′-ATCAGTTTTTGATATCAA-GCTTATACATGTCAACG-3′), and their respective internal mutagenic primers were oligonucleotides SBloop1 (5′-GATAAAGTAACAAATCCA*GATACTTCAACAC-CTGCTGCT-3′) and SBloop2 (5′-AGCAGGTGTTGAA-GTATC*TGGATTTGTTACTTTATCTCC-3′), which correspond to amino acid residues flanking the deletion region encompassing residues 163−178 (marked by *).

The altered *bla*Z gene was then resequenced using double-stranded plasmid DNA with the Sequenase Quick-Denature Plasmid DNA sequencing kit (U.S. Biochemicals, Cleveland, OH). A N-terminal methionine has been added to the engineered gene for expression. The signal peptide was not included; hence the first residue following the initiator methionine is Lys31.

The concentration of the purified protein was estimated from the absorbance of solutions at 280 nm by using the value of $\epsilon_{280} = 19\,500\ M^{-1}\ cm^{-1}$ (*30*). For storage, the protein was kept at 4 °C in solution containing 60% saturated ammonium sulfate.

Crystallization and X-ray Data Collection. Single crystals of the Ω-deletion β-lactamase were obtained at room temperature by vapor diffusion in hanging drops. The protein drops were equilibrated against reservoir solutions containing 68% saturated ammonium sulfate, 0.5% PEG 1000, and 0.3 M potassium chloride, buffered at pH 8 by 0.1 M sodium bicarbonate. The hanging drops contained equal volumes of 8.0 mg/mL enzyme and reservoir solutions. These are conditions very similar to those used to obtain crystals of the wild-type β-lactamase except that 75−78% saturated ammonium sulfate is used for the latter protein. The crystals belong to space group $P2_1$ in contrast to the *I*222 space group of the wild-type protein crystals. The unit cell dimensions are $a = 76.0$ Å, $b = 55.0$ Å, $c = 79.2$ Å, and $\beta = 90.25°$. There are two molecules in the asymmetric unit.

X-ray intensity data were collected on a Siemens area detector mounted on a Huber four-circle goniostat. Monochromated Cu Kα X-rays were generated by a Siemens rotating anode. Data to 2.3 Å resolution were collected at room temperature from a single crystal. Two orthogonal crystal orientations were scanned, each covering 190° in 0.25° oscillation steps around the goniostat's ω-axis. The data were processed with the XENGEN package (*31*). The statistics of data processing are shown in Table 1.

Structure Determination and Refinement. The structure was determined by molecular replacement using the native β-lactamase structure from which the Ω-loop was omitted

Table 1: Data-Processing Statistics

shell lower limit (Å)	no. of reflections possible	completeness (%)	redundancy	$\langle I/\sigma(I)\rangle$	R_{merge}[a]
4.18	5 014	97.2	2.4	23.8	0.078
3.32	4 915	96.3	2.2	14.9	0.103
2.90	4 900	91.2	2.1	7.5	0.150
2.63	4 873	86.0	2.0	4.2	0.213
2.44	4 874	79.1	1.8	2.8	0.270
2.30	4 822	70.0	1.3	2.0	0.320
total	29 398	86.7	2.0	10.0	0.112

[a] $R_{merge} = \sum_h\sum_i|\langle I(h)\rangle - I(h)_i|/\sum_h\sum_i I(h)_i$ for equivalent related observations.

as the search model (*8*; PDB entry code 3BLM). The program AMoRe (*32*) was used to calculate the self-rotation, cross-rotation, and translation functions. Data from 10 to 4 Å resolution were used. The cross-rotation function solution was unambiguous, with the two highest peaks (10σ and 6σ above the mean) providing the best translation search results (the highest correlation of the translation solutions was 0.557, and the correlation of the next best solution was 0.256). These were further refined by rigid body refinement to a *R*-factor value of 0.35 ($R = \sum_h||F_o| - |F_c||/\sum_h|F_o|$, where $|F_o|$ and $|F_c|$ are the observed and calculated structure factor amplitudes respectively).

The structure was refined with the program X-PLOR (*33*), employing first the simulated annealing protocol between 3000 and 300 K. This was followed by positional refinement cycles. The two molecules in the asymmetric unit were refined independently. A total of 23 263 reflections in the resolution range 7.0−2.3 Å were included in the refinement. For most of the refinement only 20 944 reflections for which $F \geq 2\sigma(F)$ were used. The cutoff on amplitudes was removed toward the end of the refinement. The progress of the refinement was evaluated by the improvement in the quality of the electron density maps and the reduced values of the conventional and free *R*-factors (*34*). During the last cycle of positional and temperature factor refinement, the data reserved for free *R* calculations were added to the refined set. The interactive graphics program TURBO−FRODO was used for map inspection and model modification (*35*). Two types of electron density maps with the coefficients $2|F_o| - |F_c|$ and $|F_o| - |F_c|$ and with calculated phases were inspected simultaneously. Solvent molecules were added once the *R*-value reached 0.21. These were assigned in the $|F_o| - |F_c|$ difference Fourier maps with a 3σ cutoff level for inclusion in the model. Solvent molecules that refined with crystallographic temperature factors larger than 60 were deleted.

Structure Analysis. Superpositions of the two protein molecules and the native structure (PDB entry code 3BLM) were calculated with the program ALIGN written by Cohen (*36*). Docking of substrates as Michaelis complexes was done manually using the interactive graphics program QUANTA (version 4.1). The X-ray structure of cephaloridine (*37*) was docked in the active site similarly to the previously docked model of ampicillin (*7*), and manual modifications were made to remove steric clashes while maintaining key interactions required for function. No energy minimization was performed.

Enzyme Kinetics. All kinetic assays were performed at 25 °C in 0.1 M potassium phosphate buffer at pH 6.8 on a Hewlett-Packard 8452A diode array spectrophotometer. The data were analyzed using the computer package SigmaPlot (Jandel Scientific). Nitrocefin was purchased from Unipath (Ogdensburg, NY). 6-β-[(Furylacryloyl)amido]penicillanic acid triethylamine salt (FAP) was purchased from Calbiochem (La Jolla, CA). Other β-lactam antibiotics were purchased from Sigma (St. Louis, MO). Hydrolysis of the chromogenic cephalosporin, nitrocefin, was monitored by the increase in absorbance at 500 nm ($\Delta\epsilon_{500} = 15\,900$ M^{-1} cm^{-1}). The hydrolysis of other substrates was monitored by loss of absorbance as follows: benzylpenicillin ($\Delta\epsilon_{232} = 940$ M^{-1} cm^{-1}), methicillin ($\Delta\epsilon_{235} = 960$ M^{-1} cm^{-1}), ampicillin ($\Delta\epsilon_{235} = 820$ M^{-1} cm^{-1}), cloxacillin ($\Delta\epsilon_{260} = 1060$ M^{-1} cm^{-1}), oxacillin ($\Delta\epsilon_{260} = 1010$ M^{-1} cm^{-1}), FAP ($\Delta\epsilon_{344} = 1330$ M^{-1} cm^{-1}), cephaloridine ($\Delta\epsilon_{260} = 10\,700$ M^{-1} cm^{-1}), cefotaxime ($\Delta\epsilon_{262} = 7250$ M^{-1} cm^{-1}), and ceftazidime ($\Delta\epsilon_{260} = 10\,200$ M^{-1} cm^{-1}).

Preincubation kinetic experiments were carried out according to the following protocol: The mutant enzyme was first incubated with an approximately 2-fold excess of the substrate for a period of 90 s. The β-lactam compounds that were preincubated with the enzyme were benzylpenicillin, ampicillin, methicillin, cloxacillin, oxacillin, cephaloridine, cefotaxime, and ceftazidime. Each mixture was added to a cuvette containing an approximately 80-fold excess of nitrocefin over enzyme, and the nitrocefin hydrolysis was monitored in the usual manner.

Mass Spectrometry. Electrospray mass spectra were obtained on a JEOL SX102 mass spectrometer equipped with an Analytica electrospray. In preparation for mass spectrometry, the ammonium sulfate and phosphate buffer containing protein sample was dialyzed against 10 mM ammonium acetate at pH 7. The acyl-enzyme complexes were formed by adding a 2-fold molar excess of β-lactam compounds to the mutant enzyme. The samples were desalted by precipitation with acetone (which denatures the protein) and analyzed in solution containing an equal volume of hexafluoro-2-propanol/ 5% acetic acid (1:1). These conditions for mass spectrometry were established in a previous study of a β-lactamase mutant (*25*). The needle voltage was maintained at approximately 5 kV. The spectra were deconvoluted using the standard software to produce charge-independent mass spectra.

Circular Dichroism. Circular dichroism (CD) spectra were measured with a Jasco 720 spectropolarimeter using a water-jacketed cylindrical cell with a path length of 1.0 mm. Temperature control was provided by a Neslab RTE-110 circulating water bath interfaced with a MTP-6 temperature programmer. The protein samples contained 0.1 M potassium phosphate buffer at pH 6.8 and 0.8 M ammonium sulfate. Far-UV CD spectra of the wild-type and the Ω-deletion β-lactamases were scanned between 200 and 250 nm at 25 °C. Three scans were averaged. Unfolding transitions were monitored at 222 nm, varying the temperature from 0 to 90 °C at a rate of 1 °C/min. After the system reached 90 °C it was cooled to its initial temperature of 0 °C, and the spectra were measured again to assess whether the unfolding is a reversible process.

RESULTS

Refined Crystal Structure. The final model of the Ω-deletion β-lactamase includes the two molecules in the asym-

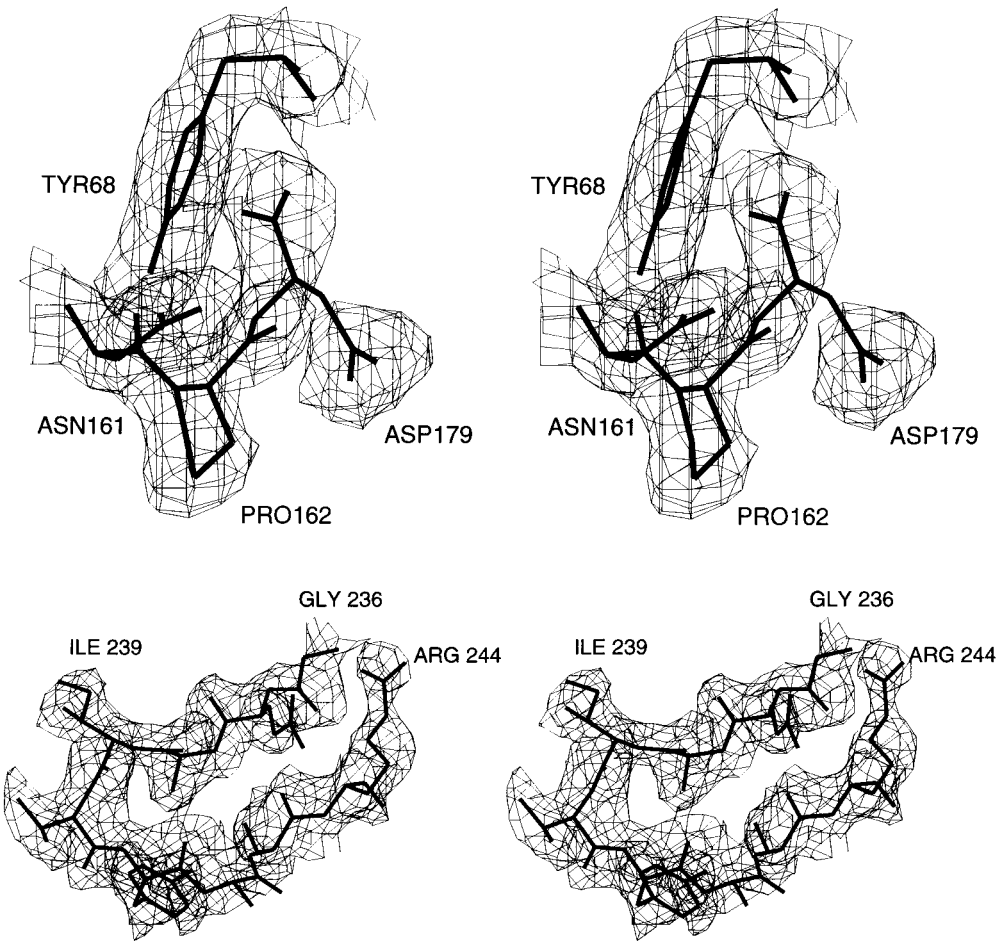

FIGURE 2: (a, top) Stereoscopic representation of the electron density map in the region where the Ω-loop was excised. The coefficients $2F_o - F_c$ and calculated phases are used. The map is contoured at the 1σ level. The deleted region is flanked by Pro162 and Asp179. The hydroxyl group of Tyr68 forms a hydrogen bond with the main chain carbonyl group of Asn161, an interaction that does not occur in the native structure. (b, bottom) Omit electron density map in a $\beta-$loop$-\beta$ region of molecule A associated with the active site, which exhibits considerable conformational difference compared with the native structure. Simulated annealing was carried out at 3000 K, omitting residues 236−244 from the model. The resulting $2F_o - F_c$ electron density map is displayed together with the final model. The map is contoured at the 1σ level. The residues are well ordered. Their average main chain crystallographic temperature factor is 17 Å^2.

metric unit. The first molecule (termed molecule A) comprises the 241 engineered amino acid residues [31−162 and 179−290 according to the Ambler et al. (*6*) numbering scheme]. The first methionine residue that was added for expression in *E. coli* is not seen in the electron density map. In the second molecule, molecule B, residue 31 is disordered and the model starts with residue 32. The model includes a total of 181 water molecules and a chloride ion. The final crystallographic *R*-factor for all data between 7.0 and 2.3 Å resolution is 0.195. The *R*-factor is 0.183 for data for which $F \geq 2\sigma F$. The *R*-free values before the reserved reflections were added to the refined set during the final stage of refinement were 0.298 for all data and 0.280 for data for which $F \geq 2\sigma F$. The root-mean-square deviations (rmsd) from ideal bond length and bond angle values of the standard geometry, compiled by Engh and Huber (*38*), are 0.018 Å and 3.4°, respectively. The overall crystallographic temperature factors (*B*-factors) of molecules A and B are 15 and 23 Å^2, respectively. The range of *B*-factors of main chain atoms in molecule A is 2−45 Å^2 (there are only 12 atoms with *B*-factor values of 2) and in molecule B 4−56 Å^2. A solvent-exposed loop region remote from the active site (residues 265−274) exhibits the highest *B*-factors in molecule B. This loop is well ordered in molecule A. Figure 2a shows the electron density at the region where the Ω-loop was deleted, confirming the expected polypeptide chain continuity between residues 162 and 179.

The overall fold of the mutant enzyme is quite similar to that of the native protein. The rmsd between α-carbon atom positions of the two molecules in the asymmetric unit and between each of these and the native protein is 0.5 Å (Figure 3). Each molecule is exposed to different crystal packing interactions, which may be responsible, in part, for some of the local structural differences observed. The space occupied by the Ω-loop in the native structure is occupied by a neighboring molecule in the Ω-loop deletion mutant's new crystal form. The intricate crystal packing affects the active site environment in the following manner: Molecule A contacts residues 99−113 of molecule B such that the amino group of Lys111 protrudes into the active site, 6.1 Å away from Ser70 O$^\gamma$. Another neighboring molecule B approaches the active site of molecule A with the carboxylate group of Asp268 forming electrostatic interactions with the active site's Tyr105 and Ser130 hydroxyl groups. The reciprocal interactions between the active site of molecule B and segments of molecule A differ. Closer contacts are formed between residues 99−113 of molecule A and the active site of molecule B, bringing the amino group of Lys111 in

FIGURE 3: Stereoscopic representation of the superposition of native β-lactamase and molecules A and B of the Ω-deletion enzyme. Virtual bonds between α-carbon atoms of the native structure are shown in solid lines, those for molecule A are shown in short broken lines, and those for molecule B are shown in long broken lines.

proximity of the Ser70 O^{γ} of molecule B (N−O distance of 4.4 Å). A second molecule A is positioned such that residues 240−241 and 270−271 cover the access to the active site of molecule B but there is no close interaction between Asp268 and the active site residues.

Two regions exhibit large conformational deviations, both between molecules A and B and between each of these and the native structure (Figures 4 and 5). Residues 236−244 form the active site's edge β-strand, the ensuing loop, and the next β-strand (Figure 2b). Residues 265−274 correspond to an adjacent $\beta-$loop$-\beta$ unit. The perturbations are larger in molecule B than in molecule A with respect to the native protein. The oxyanion hole formed by the main chain amide groups of Ser70 and Gln237 is present in molecule A but not in molecule B. Instead, the peptide bond between residues 236 and 237 is flipped such that the main chain carbonyl group of Gly236 is hydrogen bonded to the amide of Ser70 (Figure 5). Accordingly, the water molecule that occupies the oxyanion site is present in molecule A but is absent in molecule B. The $\beta-$loop$-\beta$ structural unit is perturbed in molecule B to the extent that the side chain of Arg244 is oriented toward the 265−274 loop rather than toward the active site depression (Figure 5). The distortion of the two β-strand units is accompanied by the binding of an internal solvent molecule between the main chain atoms of Gly236 and Arg244. The scattering, the broad shape of the electron density, and the nature of the electrostatic interactions with protein groups are consistent with a chloride ion (KCl was present in the crystallization solution): A distorted octahedral coordination geometry is formed with the main chain nitrogen atoms of Arg244 (3.2 Å), Asn245 (3.3 Å), Gln237 (3.8 Å), and Ala238 (3.9 Å), with the side chain nitrogen atom of Asn245 (3.4 Å), and with a water molecule (3.1 Å). The chlorine atom refined with full occupancy and a temperature factor value of 20.6 $Å^2$.

Smaller changes are associated with residues 67−68 preceding the active site Ser70, which are located close to the deleted Ω-loop. The different intermolecular environments of molecules A and B affect the orientation of the main chain carbonyl group of Asp179, and that leads to changes in the main chain conformation of Ala69. In native β-lactamase, Ala69 is sterically strained (*8*). Because of the loop deletion, the environment of Ala69 is less crowded and in molecule A it adopts an unstrained conformation. However, the packing of molecule A against molecule B leads to a crowded environment for Ala69 in molecule B, where Ala69 remains sterically strained.

Most of the active site residues, including Ser70, Lys73, Ser130, Lys234, and Asn132, are not affected by the loop deletion. The side chain of Tyr105 adopts two alternate conformations. The one in molecule A has been observed in the native structure; the one in molecule B has been observed in the structures of the clavulanate- and the phosphonate-bound enzymes (*39*, *40*). The orientation of Tyr105 in molecule B and the altered conformation of the edge β-strand bring the side chains of Tyr105 and Ile239 in close proximity to one another, which hinders access to the active site. This and the elimination of the oxyanion hole imply that molecule B has an inactive conformation.

Enzyme Activity. With the series of substrates used in this study (Figure 6), the Ω-deletion β-lactamase hydrolyzed only nitrocefin. Hydrolysis of all other substrates was undetectable. With nitrocefin, the progress curve of hydrolysis exhibits a fast initial phase followed by a slower phase (Figure 7a). The slow phase has a slight lag before reaching steady state, whereas neither burst nor lag occur with the wild-type enzyme. The amplitude of the initial burst corresponds to a stoichiometry of 1 mol of degraded nitrocefin/mol of enzyme. Note that the absorption of the acyl-enzyme is similar to that of hydrolyzed nitrocefin, and therefore the stoichiometric burst represents the formation of an acyl-enzyme rather than a complete hydrolytic cycle. The slow phase was analyzed in terms of the general integrated equation:

$$P = v_s t - (v_s - v_i)(1 - e^{-kt})/k) \qquad (1)$$

where P is the ratio of the concentration of the product to

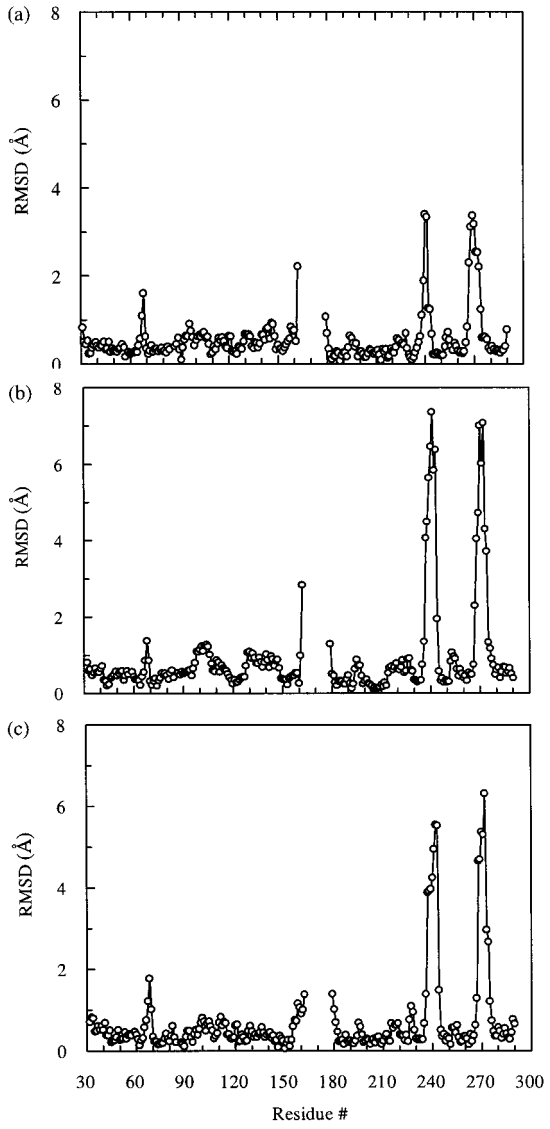

FIGURE 4: Mean main chain positional root-mean-square deviations between the molecules: (a) native β-lactamase and molecule A of the Ω-deletion enzyme; (b) native and molecule B; (c) molecules A and B. Note that residues 163−178 are not compared because of the deletion.

enzyme at time t, v_i is the initial velocity, v_s is the steady-state velocity (k_{cat}), and k is the rate constant characterizing the change corresponding to the lag.

The k_{cat} derived from the slower phase was 0.0145 s^{-1} (Table 2). The K_m was lower than 1 μM and could not be determined accurately. By comparison, the k_{cat} rate for nitrocefin hydrolysis by the wild-type enzyme is 14.0 s^{-1} and the K_m value is 7 μM (*21*, *25*).

Nitrocefin hydrolysis by the Ω-deletion β-lactamase was also followed in the presence of 1.9 M ammonium sulfate to assess whether the burst kinetics are due to purely defective deacylation apparatus or whether it is associated with substrate-induced progressive inactivation, also termed "branched pathway" (*41*). The rationale is that if partitioning between active and inactive acyl-enzyme forms occurs, a stabilizing agent such as ammonium sulfate (*42*) would decrease the conversion into the inactive acyl-enzyme and the size of the burst would increase (*19*, *43*). The burst amplitude remained 1 at high ammonium sulfate concentration, indicative of simple impairment of the deacylation machinery rather than progressive inactivation. The lag was still observed. v_i increased slightly to 0.0049 s^{-1}, and v_s increased to 0.0235 s^{-1} (Table 2). The fact that ammonium sulfate accelerates the catalytic rates of the *S. aureus* β-lactamase has been previously documented for the native, P54 mutant (D179N), and N136A β-lactamases (*21*, *25*).

The substrates that are not hydrolyzed by the Ω-deletion β-lactamase were further investigated for complex formation with the mutant enzyme. Each substrate was mixed with the enzyme, and after a preincubation period of 90 s the kinetics of nitrocefin hydrolysis were monitored. The data show that following preincubation with the traditional penicillins, benzylpenicillin and ampicillin, the activity toward nitrocefin is essentially unaltered, whereas other substrates do affect nitrocefin hydrolysis (Table 2, Figure 7b). Preincubation with penicillins with bulky side chain substituents on the β-lactam ring (methicillin, cloxacillin, and oxacillin) produced the following effects. The nitrocefin hydrolysis rates were reduced, and the lags associated with the slow phase were longer, with methicillin having a lesser impact than cloxacillin and oxacillin. The stoichiometric fast burst was eliminated after preincubation with cloxacillin and oxacillin but not with methicillin.

Preincubation with cephaloridine and with the third generation cephalosporins, cefotaxime and ceftazidime, resulted in the most dramatic changes. Both the burst and the hydrolytic activity toward nitrocefin were eliminated. The ceftazidime preincubation experiment was repeated with the wild-type enzyme because it also does not hydrolyze this compound. In contrast to the mutant enzyme, the kinetics of nitrocefin hydrolysis by the wild-type β-lactamase was unaltered, indicating that the protein does not interact tightly with ceftazidime.

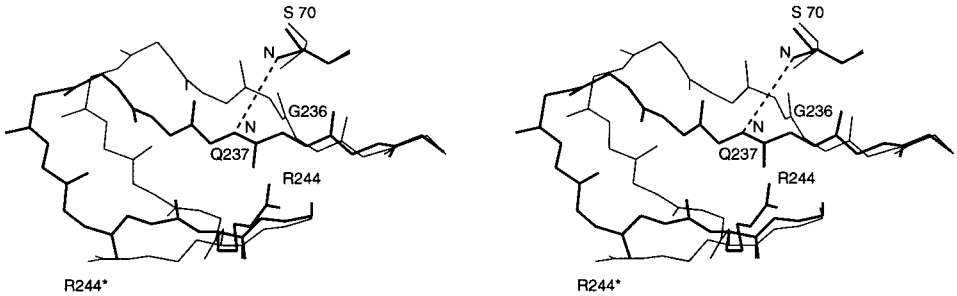

FIGURE 5: Stereoscopic representation of the conformational differences between the β−loop−β segment adjacent to the active site in molecules A (solid thick line) and B (solid thin line). Main chain atoms are shown, as well as the disposition of the side chain of Arg244 (molecule B is labeled Arg244*). The amide groups that form the oxyanion hole in molecule A are joined by a broken line. No oxyanion hole is present in molecule B. Instead, the carbonyl group of Gly236 forms a hydrogen bond with the amide of Ser70.

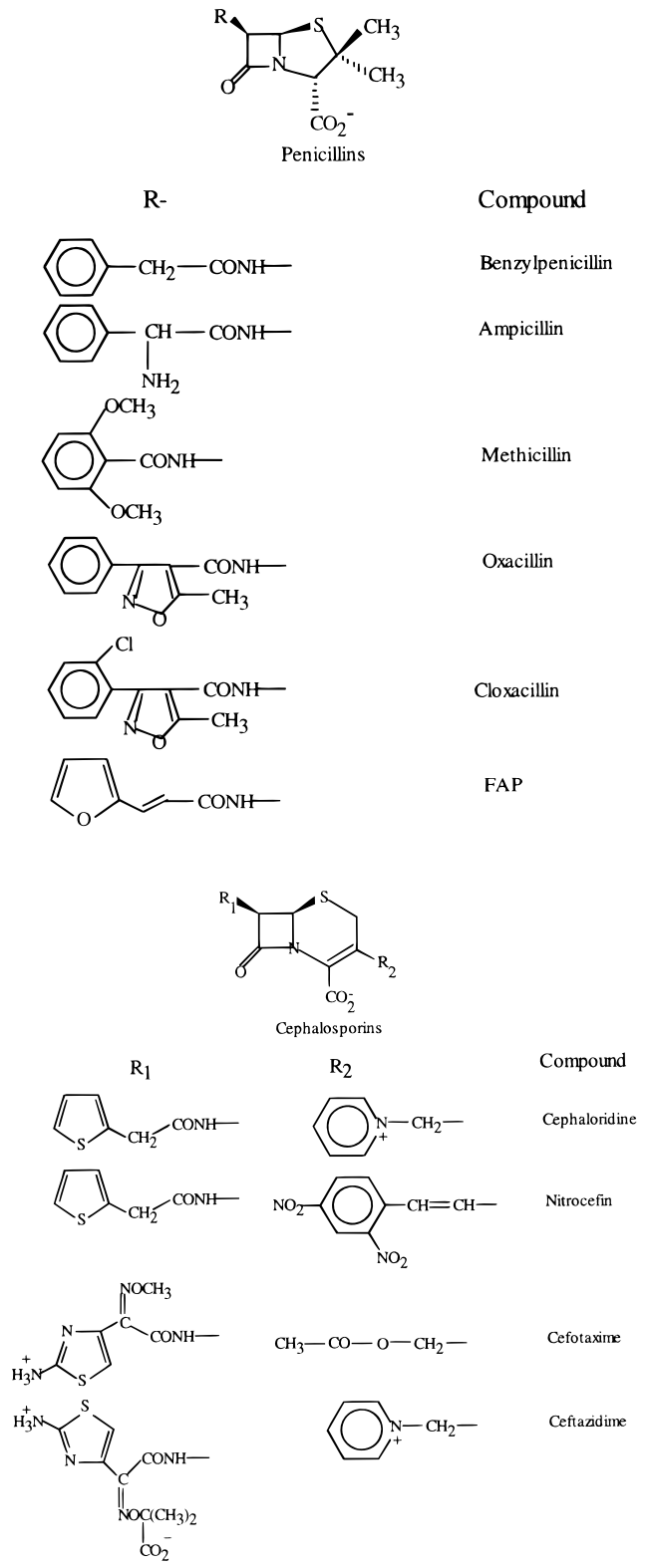

FIGURE 6: Scheme of the β-lactam antibiotics selected for this study. FAP is an abbreviation for 6-β-[(furylacryloyl)amido]-penicillanic acid.

Note that the kinetic properties of the Ω-deletion enzyme are the same as those of the N136A β-lactamase (*25*).

Mass Spectrometry of Enzyme−Cephalosporin Complexes. To determine the nature and stoichiometry of the addition products, the free Ω-deletion β-lactamase and the adducts formed with cephaloridine and cefotaxime were examined by mass spectrometry. The denaturing conditions used in the mass spectrometry experiments [acetone precipitation followed by dilution into solution of hexafluoro-2-propanol/5% acetic acid (1:1)] did not dissociate the protein−antibiotic complex; hence a covalent adduct must be formed. Previous studies of the hydrolysis of cephalosporins by β-lactamase

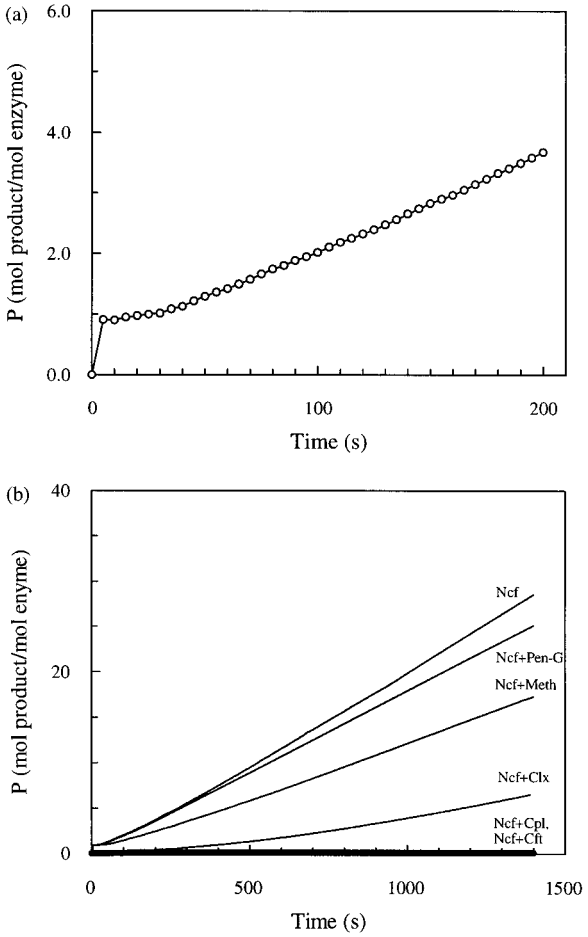

FIGURE 7: Kinetics of the Ω-deletion β-lactamase. (a) Progress curve of nitrocefin hydrolysis. The concentrations of the enzyme and nitrocefin were 1.5 and 100 μM, respectively. (b) Hydrolysis of nitrocefin (Ncf) after incubation with various β-lactam antibiotics. The preincubation period was 90 s. The concentrations of the mutant enzyme, preincubated β-lactam, and nitrocefin were 1.5, 2.7, and 100 μM, respectively. Representative members of different types of progress curves are shown: benzylpenicillin (Pen-G), methicillin (Meth), cloxacillin (Clx), cephaloridine (Cpl), and ceftazidime (Cft). See Table 2 for data on the complete set used.

Table 2: Nitrocefin Hydrolysis Rates by the Ω-Deletion β-Lactamase following Incubation with Various β-Lactam Antibiotics[a]

preincubated β-lactam	$\nu_i \times 10^2$ (s^{-1})	$\nu_s \times 10^2$ (s^{-1})	$k \times 10^2$ (s^{-1})	burst
none	0.42 ± 0.02	1.45 ± 0.02	0.95 ± 0.03	1
none, 1.9 M $(NH_4)_2SO_4$	0.49 ± 0.02	2.35 ± 0.01	0.90 ± 0.02	1
benzylpenicillin	0.36 ± 0.02	1.39 ± 0.03	1.58 ± 0.03	1
ampicillin	0.35 ± 0.01	1.36 ± 0.02	1.54 ± 0.04	1
methicillin	0.20 ± 0.01	1.22 ± 0.01	0.86 ± 0.04	1
oxacillin	0.07 ± 0.01	1.10 ± 0.02	0.18 ± 0.01	
cloxacillin	0.07 ± 0.01	1.06 ± 0.04	0.16 ± 0.02	
cephaloridine	0	0	0	
ceftazidime	0	0	0	
cefotaxime	0	0	0	

[a] The errors associated with the fit to the general integrated equation are provided.

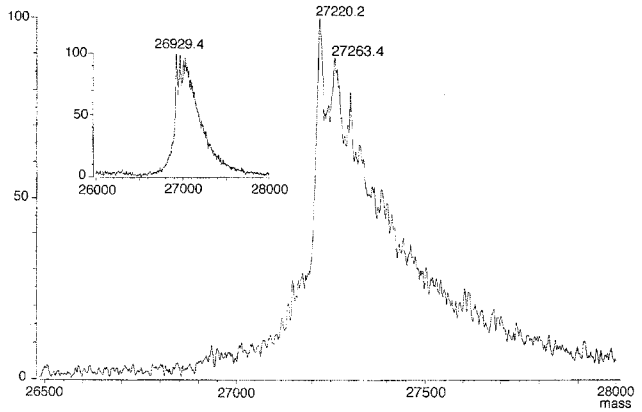

FIGURE 8: Mass spectrum of the adduct formed between cephaloridine and the Ω-deletion β-lactamase. The protein solution was desalted and mixed with an equal volume of hexafluoro-2-propanol/5% acetic acid (1:1). The predicted mass of the adduct after 3′-substituent elimination was 27 262.2 units, and the measured peak was at 27 263.4 units. In addition, decarboxylation occurred, resulting in a peak with 43 lower mass units. The spectrum confirms that only a 1:1 antibiotic/protein adduct is formed. The inset shows the free protein (calculated mass 26 926.2, observed mass 26 929.4).

from *S. aureus* PC1 concluded that the 3′-substituents (R_2 in Figure 6) of cephalosporins may be eliminated prior to deacylation (*44*). The mass shifts predicted for the cephaloridine and cefotaxime if no elimination of the 3′-substituent occurs are 415 and 455 units, respectively. After elimination, the expected mass shifts are 336 and 396 units, respectively. The free protein was measured at 26 929.4 mass units (calculated mass 26 926.2) and the measured masses of the cephaloridine and cefotaxime adducts were 27 263.4 and 27 325.4, respectively (the calculated masses for 3′-substituent elimination are 27 262.2 and 27 322.2). An additional peak was obtained in each experiment, at 43 and 41 mass units lower than the peaks corresponding to the covalent adducts that were undergoing the 3′-substituent elimination (27 220.2 and 27 284.4 mass units for cephaloridine and cefotaxime, respectively). These were attributed to decarboxylation adjacent to the 3′-group in the mass spectrometer (predicted loss of 44 mass units). The result for cephaloridine is shown in Figure 8.

DISCUSSION

Structural Consequences of the Loop Deletion. The deletion of the Ω-loop eliminates the key catalytic residue, Glu166. That obviously leads to impaired deacylation. The deletion also exposes internal residues to solvent. Several of these internal residues are hydrophilic and support the inclusion of the internal solvent molecules in the native structure of the *S. aureus* enzyme. Therefore, no large hydrophobic patch is exposed to solvent by the deletion. Protein stability, as estimated from the denaturation profile in the CD, remains the same as that of the wild-type β-lactamase. As reported previously for the wild-type enzyme (*25*) the mutant protein unfolds at 74 °C. In both cases the unfolding profiles fit two-step transitions, but the process leads to aggregation and is irreversible in that after cooling the sharp transition disappears.

The absence of the Ω-loop enlarges the active site. That provides the adjacent structural units with new degrees of conformational flexibility. The β−loop−β unit closest to the Ω-loop in the native structure (residues 236−244) undergoes the most significant changes, which then propagate further to the adjacent β−loop−β unit (residues *265*−*274*). The two molecules in the asymmetric unit may exhibit altered conformations because of the different packing constraints of the crystal lattice. In light of these two views of the molecule, it becomes clear that the presence of the Ω-loop restricts the disposition of the edge β-strand, preventing it from occupying space that is required for substrate binding. When the loop is absent, the β-strand can sample different conformations and collapse toward the active site space. In addition, the oxyanion hole is not formed in molecule B. As this is a key feature of β-lactam binding, molecule A represents better the active form of the mutant enzyme. Thus, models of Michaelis complexes have been developed using the structure of molecule A.

The sterically strained main chain dihedral angle of Ala69 in the native structure facilitates the contact between the active site helix to the edge β-strand and restricts the flexibility of the oxyanion hole. The Ω-loop plays a key role in these steric restrictions. When the loop is deleted, the environment of Ala69 is less crowded and the steric strain can be relieved, leading to adjustments of the oxyanion hole such that the distance between the two NH groups is 0.85 Å longer than that seen in the native oxyanion hole. Such changes may impact both the kinetics and the specificity of the enzyme.

Enzyme Activity. The crystal structure confirms that the Ω-deletion β-lactamase adopts a unique fold which preserves the spatial arrangement of part of the catalytic apparatus. How does this correlate with function?

Using mechanism-based inhibitors, it has been established that the hydrolysis of β-lactam compounds by the class A β-lactamases involves an acyl-enzyme intermediate (*2*−*5*). The simplest mechanism that accounts for the acyl-enzyme intermediate is shown in Scheme 1, where the enzyme, substrate, and product are represented by E, S, and P, respectively, ES denotes the Michaelis complex, and EC denotes the acyl-enzyme complex.

Scheme 1

$$E + S \overset{K_s}{\longleftrightarrow} ES \xrightarrow{k_2} EC \xrightarrow{k_3} E + P$$

With the exception of nitrocefin, the Ω-loop deletion abolishes the ability of the enzyme to hydrolyze β-lactam compounds. For nitrocefin, a fast initial burst corresponds to the appearance of a stoichiometric amount of acyl-enzyme. The magnitude of the burst is not affected by the addition of ammonium sulfate, ruling out the kinetic scheme of a branched pathway mechanism corresponding to substrate-induced progressive inactivation (*19*, *25*, *41*, *43*). Following the burst, the slower phase reflects the incompetence of the mutant enzyme to undergo deacylation because of the missing Glu166 (Figure 7a). The slow phase exhibits a short lag, suggestive of a substrate-induced activation. Because the lag is subtle, and for the sake of simplicity, the kinetics of nitrocefin hydrolysis will be treated according to Scheme 1.

The burst and the steady-state hydrolytic rate for nitrocefin are similar to those measured with three other mutant β-lactamases: D179N (termed P54) (*21*), N170Q (*19*), and

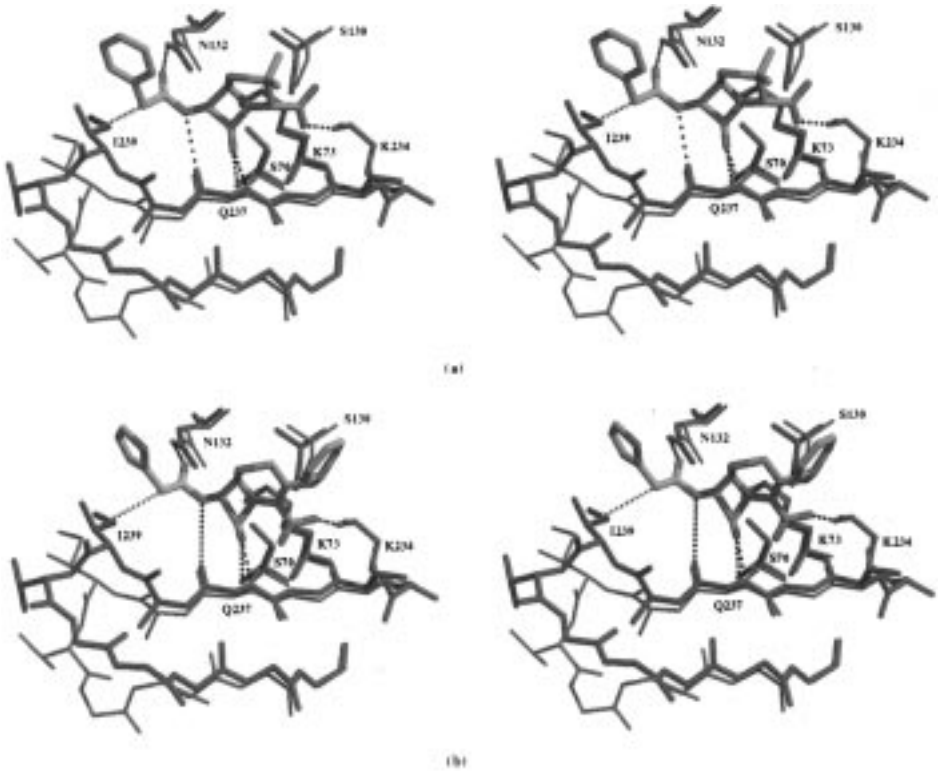

FIGURE 9: Stereoscopic view of the superposition of the active sites of the native β-lactamase (red) and molecule A of the Ω-deletion (blue) β-lactamase, together with modeled drugs (shown in atomic colors). The hydrogen-bonding interactions are shown as dotted black lines. The steric interaction between the Ile239 C^{β} atom and the drug is shown in dotted magenta lines. (a) Docked benzylpenicillin. The distance between the Ile239 C^{β} atom of the mutant enzyme and C^{17} of benzylpenicillin is 1.8 Å (native 3.3 Å).The failure of the mutant enzyme to be acylated by penicillins is attributed to a shift in the edge β-strand that leads to steric clashes. (b) Docked cephaloridine. The distance between the marked atoms is 2.9 Å (native 3.4 Å).

N136A (*25*). With the first mutant enzyme, an invariant salt bridge between Asp179 and Arg164, at the bottom of the Ω-loop, has been eliminated. Consequently, part of the loop including Glu166 is disordered and deacylation is impaired. In the second mutant enzyme, N170Q, the site of the hydrolytic water molecule has been blocked by the glutamine, also leading to impaired deacylation. Finally, by the mutation N136A, important interactions with the main chain amide and carbonyl groups of Glu166 are removed, destabilizing the ensuing non-proline *cis* peptide bond. This may lead to the disorder of the Ω-loop. The kinetic consequences of the N136A mutation and the Ω-deletion are more severe than those of the D179N or N170Q replacements. Whereas the hydrolysis rate of benzylpenicillin by the D179N and N170Q β-lactamases is substantially reduced, but is still measurable, the N136A and the Ω-deletion mutant enzymes do not hydrolyze any of the β-lactams that have been studied except for nitrocefin. For N136A β-lactamase we proposed that the productive conformation of the Ω-loop is not sampled at all. The proposal is supported by the structure and kinetics of the current enzyme variant that does not carry the loop.

A single acylation step is undetectable in assays using β-lactam antibiotics with low extinction coefficients measured at wavelengths where the protein absorbs strongly. Therefore, the nitrocefin activity was used to indirectly assess whether these compounds form complexes with the Ω-deletion enzyme. Nitrocefin was used previously as a reporter substrate for β-lactam compounds that inactivate β-lactamases (*25, 45, 46*). As with the N136A mutant β-lactamase, for those β-lactams that form stable acyl-enzyme complexes, incubation of the compounds with the protein in close to stoichiometric amounts, followed by assaying for nitrocefin activity, should be manifested by elimination of nitrocefin hydrolysis. The caveat is that a very tight noncovalent complex may also produce the same kinetic effect. Performing the mass spectrometry under denaturing conditions distinguished between the two possibilities.

For the series of β-lactam antibiotics used, elimination of nitrocefin hydrolysis occurred with the traditional cephalosporin, cephaloridine, and with the third generation cephalosporins, cefotaxime and ceftazidime (Figure 7b, Table 2). A control experiment with the wild-type enzyme showed that nitrocefin hydrolysis is unaffected by preincubation with ceftazidime, confirming that in that case ceftazidime does not form a stable acyl-enzyme.

Electrospray mass spectrometry revealed adducts with stoichiometry of 1:1 between the mutant protein and the cephalosporin compounds. All experiments were carried out under denaturing conditions, when a noncovalent complex would dissociate. Therefore, tight noncovalent complexes that do not proceed to form acyl-enzyme complexes have been ruled out, and the formation of such complexes with either first or third generation cephalosporins has been confirmed.

A question remains, why do all four mutant enzymes, D179N, N170Q, N136A, and the Ω-deletion, exhibit similar slow turnovers of nitrocefin while deacylations of other substrates are more severely impaired? This points at the possibility of an alternative deacylation mechanism for nitrocefin, perhaps because the acyl-enzyme complexes with nitrocefin are chemically unstable, enabling a less nucleo-

philic water molecule to play the hydrolytic role.

The penicillins with flexible side chain substituents, benzylpenicillin and ampicillin, are the best substrates of native β-lactamase from *S. aureus* PC1. Yet, as there is no effect on nitrocefin hydrolysis by the mutant enzyme, they are incapable of forming either tight Michaelis complexes or stable acyl-enzyme adducts. On the other hand, the reduction in the nitrocefin hydrolysis rate after incubation with penicillins with bulky side chain substituents, cloxacillin, oxacillin, and methicillin, indicates that these form noncovalent slowly dissociating complexes. The effect is most pronounced with cloxacillin and oxacillin and less so in the presence of methicillin. In addition, the initial stoichiometric burst is eliminated following the incubation with cloxacillin and oxacillin but not with methicillin, a compound with the least bulky side chain substituent of this class of penicillins.

The preincubation results are identical to those observed with the N136A β-lactamase. The active sites of both mutant enzymes recognize first and third generation cephalosporins rather than penicillins. For acylation, these mutant enzymes exhibit altered specificity compared with the wild-type enzyme, and the similarity between the two provides further support to the proposal that the Ω-loop in N136A β-lactamase is disordered and Glu166 is never in the position required for enhancing the nucleophilicity of the hydrolytic water molecule.

Structural Basis for Altered Specificity. As discussed earlier, molecule A of the asymmetric unit of the crystal represents better the active conformation of the Ω-deletion enzyme. Therefore, it was used as the framework for modeling the binding of benzylpenicillin and cephaloridine. The modeled complexes could then be compared with the respective models of the wild-type β-lactamase, providing a structural rationale for the activity of the mutant enzyme toward cephalosporin compounds and its failure to act on penicillin compounds. Superposition of the β−loop−β units of the mutant and wild-type enzymes and key catalytic residues that play a role in binding and acylation highlights the differences that may lead to the altered specificity (Figure 9). Ala238 and Ile239 in the mutant enzyme occupy active site space that is free in the wild-type enzyme because of the constraint imposed on the β−loop−β unit by the presence of the Ω-loop. For productive binding (i.e., acylation), the carbonyl oxygen atom of the β-lactam antibiotics should be located in the oxyanion hole, and the carbon atom should be accessible for nucleophilic attack by the hydroxyl group of Ser70. At the same time, the invariant carboxylate moiety on the ring that is fused to the β-lactam ring should form an ion pair interaction with Lys234 to prevent buried unbalanced charges. The relative orientations of the β-lactam's carbonyl and carboxylate groups differ in penicillins and cephalosporins, and therefore the two fused rings are expected to dock in a slightly different manner. Moreover, the relative orientation of the carboxylate group and the β-lactam side chain substituent is different in the two types of antibiotics. As shown in Figure 9, with the appropriate interactions of the β-lactam carbonyl and carboxylate groups, the side chain substituent of the benzylpenicillin forms too short contacts with Ile239 (1.8 Å between the C^{β} atom of Ile239 and C^{17} of benzylpenicillin), whereas the respective side chain of the cephaloridine is accommodated in the active site without steric clashes.

In general, cephalosporin antibiotics are hydrolyzed by class C β-lactamases better than they are hydrolyzed by the class A enzymes. Lobkovsky et al. (*47*) proposed that the difference in activity arises from a loop in the class C β-lactamase that occupies approximately the same space as that occupied by the Ω-loop in the class A enzymes, but is recessed compared with the Ω-loop. This leads to different positions of the respective active site edge β-strands. Superposition of the structures of the class C enzyme and of the Ω-loop deletion enzyme reveals that the edge β-strands of the two molecules do not fit well. Hence, the structural basis for the preference for cephalosporins in the class C enzyme and in the Ω-loop deletion mutant may not be the same.

Finally, in addition to the altered β-lactam antibiotics recognition profile, the absence of the Ω-loop also accounts for the ability of the mutant enzyme to be acylated by third generation cephalosporins. The geometry of the cephalosporin enables it to be accommodated in the active site, and the bulky side chain typical of the third generation cephalosporins can adjust so that it occupies the space created by deletion of the loop. This model leads to the possibility that a new deacylation apparatus may be engineered into the Ω-deletion β-lactamase, generating a new variant enzyme, resistant to third generation cephalosporins.

ACKNOWLEDGMENT

We thank Drs. John Moult and Edward Eisenstein for useful discussions.

REFERENCES

1. Ambler, R. P. (1980) *Philos. Trans. R. Soc. London B289*, 321−331.
2. Knott-Hunziker, V., Waley, S. G., Orlek, B. S., and Sammes, P. G. (1979) *FEBS Lett. 99*, 59−61.
3. Cartwright, S. J., and Coulson, A. F. W. (1980) *Philos. Trans. R. Soc. London B289*, 370−372.
4. Cohen, S. A., and Pratt, R. F. (1980) *Biochemistry 19*, 3996−4003.
5. Fisher, J., Belasco, J. G., Kohsla, S., and Knowles, J. R. (1980) *Biochemistry 19*, 2895−2901.
6. Ambler, R. P., Coulson, A. F. W, Frère, J.-M., Ghuysen, J.-M., Joris, B., Forsman, M., Levesque, R. C., Tiraby, G., and Waley, S. G. (1991) *Biochem. J. 276*, 269−270.
7. Herzberg, O., and Moult, J. (1987) *Science 236*, 694−701.
8. Herzberg, O. (1991) *J. Mol. Biol. 217*, 701−719.
9. Moews, P. C., Knox, J. R., Dideberg, O., Charlier, P., and Frère, J.-M. (1990) *Proteins 7*, 156−171.
10. Knox, J. R., and Moews, P. C. (1991) *J. Mol. Biol. 220*, 435−455.
11. Jelsch, C., Lenfant, F., Masson, J. M., and Samama, J. P. (1992) *FEBS Lett. 299*, 135−142.
12. Jelsch, C., Mourey, L. F., Masson, J. M., and Samama, J. P. (1993) *Proteins 16*, 364−383.
13. Strynadka, N. C. J., Adachi, H., Jensen, S. E., Johns, K., Sielecki, A., Betzel, C., Sutoh, K., and James, M. N. G. (1992) *Nature 359*, 700−705.
14. Herzberg, O., and Moult, J. (1991a) *Curr. Opin. Struct. Biol. 1*, 946−953.
15. Gibson, R. M., Christensen, H., and Waley, S. G. (1990) *Biochem. J. 272*, 613−619.
16. Oefner, C., D'Arcy, A., Daly, J. J., Gubernato, K., Charnas, R. L., Heinze, I., Hubschwerlen, C., and Winkler, F. K. (1990) *Nature 343*, 284−288.
17. Lobkovsky, E., Billing, E. M., Moews, P. C., Rahil, J., Pratt, R. F., and Knox, J. R. (1994) *Biochemistry 33*, 6762−6772.

18. Damblon, C., Raquet, X., Lian, L.-Y., Lamotte-Brasseur, J., Fonze, E., Charlier, P., Roberts, G. C. K., and Frère, J.-M. (1996) *Proc. Natl. Acad. Sci. U.S.A.* 93, 1747−1752.
19. Zawadzke, L. E., Chen, C. C. H., Banerjee, S., Li, Z., Wäsch, S., Kapadia, G., Moult, J., and Herzberg, O. (1996) *Biochemistry 35*, 16475−16482.
20. Knox, J. R., Moews, P. C., and Frère, J.-M. (1996) *Chem. Biol. 3*, 937−947.
21. Herzberg, O., Kapadia, G., Blanco, B., Smith, T., and Coulson, A. F. W. (1991) *Biochemistry 30*, 9503−9509.
22. Adachi, H., Ohta, T., and Matsuzawa, H. (1991) *J. Biol. Chem. 266*, 3186−3191.
23. Escobar, W. A., Tan, A. K., and Fink, A. L. (1991) *Biochemistry 30*, 10783−10787.
24. Guillaume, G., Vanhove, M., Lamotte-Brasseur, J., Ledent, P., Jamin, M., Joris, B., and Frère, J.-M. (1997) *J. Biol. Chem. 272*, 5438−5444.
25. Banerjee, S., Shigematsu, N., Pannell, L. K., Ruvinov, S., Orban, J., Schwarz, F., and Herzberg, O. (1997) *Biochemistry 36*, 10857−10866.
26. Herzberg, O., and Moult, J. (1991b) *Proteins: Struct., Funct., Genet. 11*, 223−229.
27. Craig, S., Hollecker, M., Creighton, T. E., and Pain, R. H. (1985) *J. Mol. Biol. 185*, 681−687.
28. Zawadzke, L. E., Smith, T., and Herzberg, O (1995) *Protein Eng. 8*, 1275−1285.
29. Ho, S. N., Hunt, H. D., Horton, R. M., Pullen, J. K., and Pease, L. R. (1989) *Gene 77*, 51−59.
30. Carrey, E. A., and Pain, R. H. (1978) *Biochim. Biophys. Acta 533*, 12−22.
31. Howard, A. J., Gilliland, G. L., Finzel, B. C., Poulos, T., Ohlendorf, D. O., and Salemme, F. R. (1987) *J. Appl. Crystallogr. 20*, 383−387.
32. Navaza, J. (1994) *Acta Crystallogr. A50*, 157−163.
33. Brünger, A. T. (1992a) *X-PLOR version 3.1, a system for X-ray crystallography and NMR*, Yale University Press, New Haven and London.
34. Brünger, A. T. (1992b) *Nature 355*, 472−475.
35. Roussel, A., and Cambillau, C. (1989) *Silicon Graphics Directory*, Silicon Graphics, Mountain View, CA.
36. Satow, Y., Cohen, G. H., Padlan, E. A., and Davies, D. R. (1986) *J. Mol. Biol. 190*, 593−604.
37. Sweet, R. M., and Dahl, L. F. (1970) *J. Am. Chem. Soc. 92*, 5489−5495.
38. Engh, R. A., and Huber, R. (1991) *Acta Crystallogr. A47*, 392−400.
39. Chen, C. C. H., and Herzberg, O. (1991) *J. Mol. Biol. 224*, 1103−1113.
40. Chen, C. C. H., Rahil, J., Pratt, R. F., and Herzberg, O. (1992) *J. Mol. Biol. 234*, 165−178.
41. Waley, S. G. (1991) *Biochem. J. 279*, 87−94.
42. Mitchinson, C., and Pain, R. H. (1985) *J. Mol. Biol. 184*, 331−342.
43. Escobar, W. A., Tan, A. K., Lewis, E. R., and Fink, A. L. (1994) *Biochemistry 33*, 7619−7626.
44. Faraci, W. S., and Pratt, R. F. (1985) *Biochemistry 24*, 903−910.
45. Galleni, M., and Frère, J.-M. (1988) *Biochem. J. 255*, 119−122.
46. Matagne, A., Misselyn-Bauduin, A.-M., Joris, B., Erpicum, T., Granier, B., and Frère, J.-M. (1990) *Biochem J.* 265, 131−146.
47. Lobkovsky, E., Moews, P. C., Liu, H., Zhao, H., Frère, J.-M., and Knox, J. R. (1993) *Proc. Natl. Acad. Sci. U.S.A. 90*, 11257−11261.

BI972127F